J Mater Sci (2018) 53:11253–11264

Chemical routes to materials

Fabrication of superhydrophobic coating from non-fluorine siloxanes via a one-pot sol–gel method

Xiaodan Chen[1,2,3], Yufang Chen[1,3], Tao Jin[1,3,*], Li He[1,2], Yu Zeng[3], Qian Ma[3], and Na Li[3]

[1] Guangzhou Institute of Chemistry, Chinese Academy of Sciences, Guangzhou 510650, People's Republic of China
[2] University of Chinese Academy of Sciences, Beijing 10049, People's Republic of China
[3] Guangzhou CAS Test Technical Services Co., Ltd, Guangzhou 510650, People's Republic of China

Received: 14 November 2017
Accepted: 18 April 2018
Published online: 23 May 2018

ABSTRACT

To fabricate a superhydrophobic and durable coating, non-fluorine siloxane solution for the coating was successfully synthesized via a facile one-pot method. The wetting properties and morphology of coatings with different concentration and adding time of additives were studied. Under condition of low water content, the coatings' superhydrophobicity was improved with the increasing amount of ammonia content, water content, and low-surface-energy material (HTMS) content. However, too more ammonia or water or HTMS would sacrifice the coating's integrality and lead to the cracking of it. The obtained coatings showed good superhydrophobicity and anti-UV property on plain and even curved substrates, including glass, metal, and polymer. Contact angle and sliding angle of the coating could reach 158° and 1.8°, respectively. What is more, coating on PET filter could be used for oil/water separation with an efficiency of 80%.

Introduction

Superhydrophobic surfaces that exhibit very high water contact angle (CA, greater than 150°) and very low roll-off angle have received much attentions due to their huge potential application in environment, energy and biomedical fields [1, 2]. Among artificial superhydrophobic coatings, those with durability could be widely applied in self-clean or icephobic [3] outdoor instruments' coatings [4–6], anti-corrosion, and anti-biological adhesion, etc. [7–10]. To date, a great deal of effort has been made to fabricate coatings, possessing the properties of superhydrophobicity and durability. Basically, hierarchical surface structure and low-surface-energy materials are both essential for the preparation of superhydrophobic surfaces [11–14]. Recent process [15] in obtaining hierarchical structure contain template-based techniques [16, 17], etching [18, 19], deposition [20–22], electrospinning [23, 24], sol–gel [25–27], and phase separation [28, 29], etc. Meanwhile, low-surface-energy materials, such as fluoride, hydrophobic polymer, and compounds with alkyl groups, have been utilized to make surfaces more hydrophobic. In

Address correspondence to E-mail: jintao@gic.ac.cn

https://doi.org/10.1007/s10853-018-2348-7

these studies, sol–gel techniques have been widely used because of its mild operation situations without extra post-treatments such as high-energy etching or high-temperature calcination. In addition, the surfaces morphology can be easily controlled and coatings' properties can be enhanced with constituent oxide materials during sol–gel process [30]. Nevertheless, the drawback of particles aggregation due to high surface-energy in sol–gel technique has greatly restricted its applications in the required fields [31]. To overcome this shortcoming, several approaches have been developed, especially the kinetic reaction controlling or introducing surface modifiers. However, many corresponding fabrication crafts are unstable and complicated, and the guiding rules are still unclear [32, 33].

In this study, we have obtained superhydrophobic surfaces in a simple way with non-fluorine siloxanes including tetraethyoxysilane (TEOS), 3-(methacryloyloxy) propyltrimethoxysilane (MPS, commercial name: Silane A174), and hexadecyltrimethoxysilane (HTMS). Herein, TEOS as precursor, and MPS as co-precursor to improve the dispersion of formed particles, were first hydrolyzed into silanol with the help of ammonia and gradually formed three-dimensional silica network via dehydration condensation reaction. And then HTMS containing three hydrolysable methoxy groups and long-chain alkane, which underwent hydrolysis and condensation reactions with TEOS and MPS, further improved the roughness of the surface and provided hydrophobic group for the superhydrophobic coatings. The obtained modified silica sol was stable and could form superhydrophobic coatings with anti-UV property on different kinds of substrates such as glass, metal, and polymer. Contact angle and sliding angle of the coating could reach 158° and 1.8°, respectively. What is more, coating on PET filter could be used for oil/water separation with an efficiency of 80%. None pre- or post-treatment was required in the synthesis process.

Experimental

Materials

Tetraethyoxysilane (TEOS, 99%), 3-(methacryloyloxy) propyltrimethoxysilane (MPS, 99%), hexadecyltrimethoxysilane (HTMS, 99%), NH_4OH (28% NH_3 in H_2O), absolute ethanol (EtOH, AR), isopropyl alcohol (IPA, AR) were purchased from Aladdin Industrial Co., Ltd (Shanghai, China). All chemicals were used as received without further purification.

PET nonwovens (50 g/cm^2) were supplied by Baoji Jiaxin Filter Materials Technologies Co., Ltd (Shaanxi, China, commercial name: J50), and the other substrates for superhydrophobic coatings were acquired from supermarket. Deionized water was used in all experiments.

Synthesis of organic–inorganic hybrid silica sol

Organic–inorganic hybrid silica sol was synthesized by a one-pot method, and the corresponding synthetic route referencing to Stöber [34] method was as follows: 1.663 g TEOS, 5 g H_2O, and 45 g EtOH were successively added under magnetic stirring into a 250-mL three-necked round-bottomed flask matched with a condenser, and blended at 30 °C for 30 min. The obtained solution was followed by the addition of 1.167 g MPS dropwise and stirred for 1 h, after that a given amount of ammonia was added and then the mixed solution was stirred for another 4 h. Finally, a solution containing 0.909 g HTMS, 4 mL IPA, and 2 mL EtOH was put into the reaction flask with temperature raising to 75 °C for another 5-h hydrolysis to obtain the modified silica sol for coatings.

Preparation of superhydrophobic surfaces

The obtained silica nano-sol was directly used to form surface coatings on different kinds of substrates like glass slide, metal, and polymer. The slide was hydroxylation by plasma treatment, and all surfaces were coated by means of self-leveling coating and fiber by dip-coating. Obtained coatings were heated and consolidated at 60 °C for 12 h. The following related tests and characterizations are based on slides.

Characterization

Water contact angle (CA) and sliding angle (SA) were measured by contact angle measuring instrument (JC2000D2, Shanghai Zhongchen Digital Technology Co., Ltd). A water droplet of 5 μL was employed, and each contact angle value was an average of five measurements on different positions of the coating.

Sliding angles were also measured five times for each sample by tilting the coating until the droplet (5 μL) began to slide. FTIR spectra of the samples were recorded by a Bruker Tensor 27 FTIR spectrophotometer. Morphology of the coating surfaces was investigated by using a Hitachi S3400N scanning electron microscope (SEM) and Bruker Multimode 8 atom force microscope (AFM).

Results and discussion

Real-time study of wettability and morphology of coatings on slides and FTIR characterization

For real-time monitoring of the surfaces' wetting properties, modified silica sol were taken out from time to time during the synthesis process and self-level on slides and water contact angle and morphology were studied. Figure 1 shows the change in water contact angle with different HTMS adding moments, and Fig. 2a–d shows the related coating surfaces' morphology characterized by means of SEM and AFM. It can be evidently observed that water contact angle significantly rose up from 51° to 158° with the increase of HTMS adding time. Before HTMS adding in (considered HTMS adding moment as 0 and used negative abscissa to indicate moment before HTMS adding in), the coating was hydrophilic with a contact angle of 51° and the surface was not rough enough with large sticky sphere particles (Fig. 2a, a-1) due to severe aggregation, and the corresponding coating's root mean roughness (Rq) was 93.5 nm. With the addition of HTMS, the long-chain alkyl groups of HTMS improved the dispersion of particles as well the hydrophobicity of the coating and the contact angle was raised to 110°. As reaction going on, the particles first became slightly smaller and the corresponding coating's roughness also became slightly smaller with Rq of 73.9 nm (Fig. 2b, b-1). After that, the small particles gradually packed up (Fig. 2c, c-1) because of the condensation reaction, as a result, the corresponding coating got rougher with Rq of 133 nm. After adding HTMS for 5 h, a kind of continuously hierarchical structure with small roughness of 114 nm was obtained (Fig. 2d, d-1), and hydrophobicity of coatings became stable with almost constant contact angle at 158°. Therefore, we believed that continuously hierarchical structure was more conducive to the hydrophobicity of coatings.

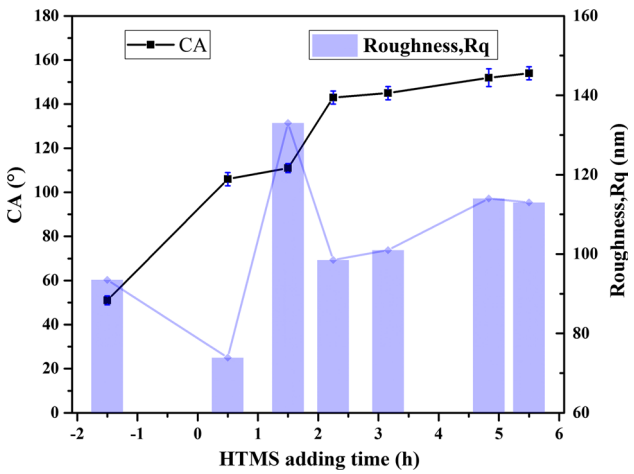

Figure 1 Water contact angle and root mean roughness of different HTMS adding time.

To further investigate the chemical structure, the coating surfaces before and after HTMS adding were characterized by FTIR, which is shown in Fig. 3. It is observed that the strong absorption peak at 3452 cm^{-1} is attributed to the vibrations of –OH on the sample of before HTMS adding, and it becomes very weak on the sample after HTMS adding, which indicates Si–OCH_3 group was successfully hydrolyzed to Si–OH first and then condensed to Si–O–Si [35, 36]. Besides, the characteristic peak centered at 2927.4 and 2856.1 cm^{-1} assigning to –CH_3 and –CH_2– of HTMS could be found in the sample after HTMS adding, while the peak at 1456 cm^{-1} corresponding to the CH_2 of HTMS becomes stronger after HTMS adding in; meantime, that at 1384.6 cm^{-1} assigned to CH_3 of MPS gets weak. Therefore, the long-chain alkane of HTMS was successfully covalently connected to the Si–O–Si network.

Thus, the whole process could be schemed as in Fig. 4. Before HTMS adding in, the coating was hydrophilic with unresponsive –OH and methacryloxypropyl group of MPS on a not-so-rough surface. Later, with HTMS adding in for appropriate reaction time, many –OH groups were grafted by long-chain alkane of HTMS, which leaded to good dispersion of the sample and rough surface of the surface morphology; thus, the coating got superhydrophobic.

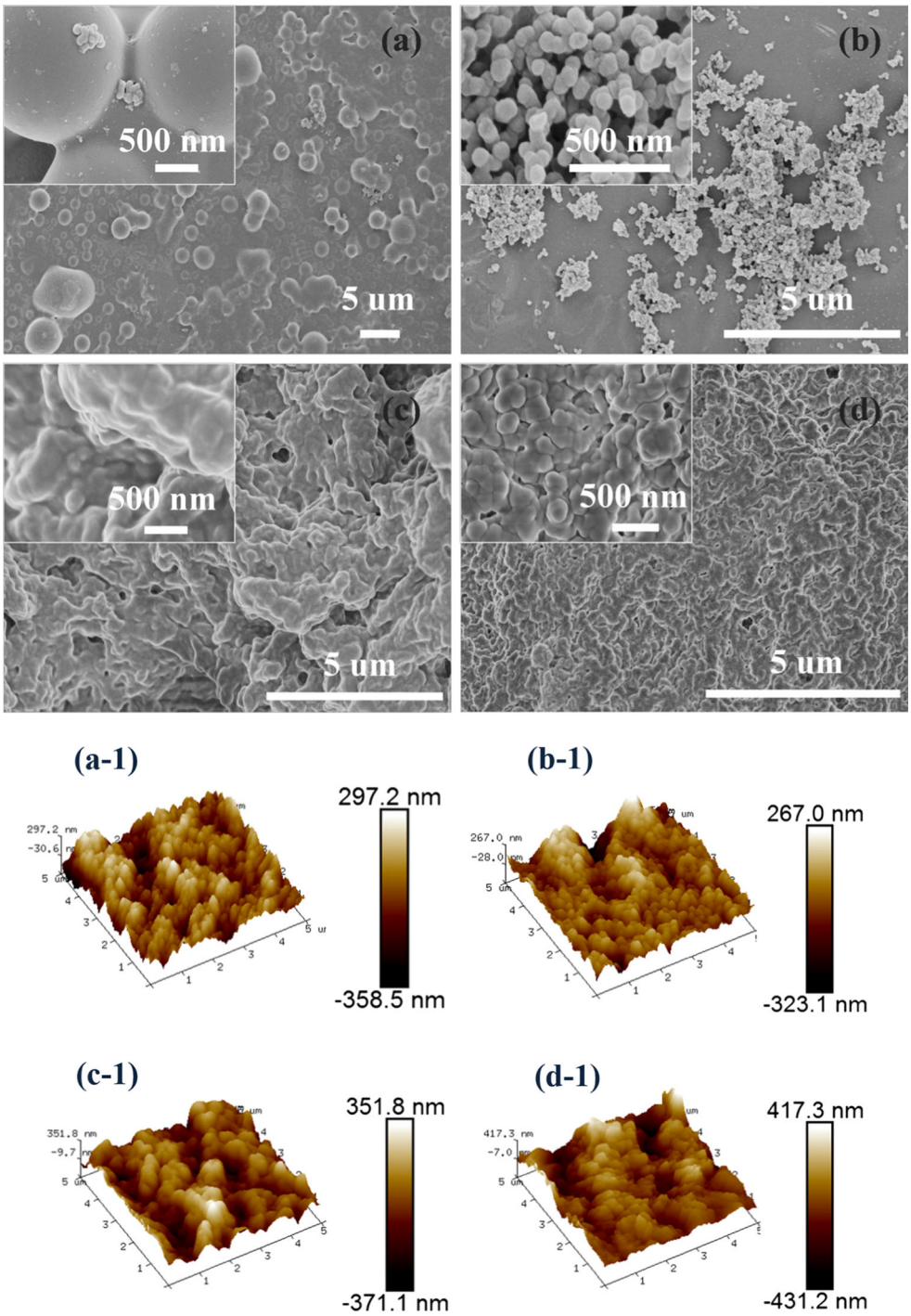

Figure 2 Morphology via SEM of coatings with different HTMS adding times of **a** − 1.5 h; **b** 1 h; **c** 2.5 h; **d** 5.5 h. Morphology via AFM of coatings with different HTMS adding times of **a-1** − 1.5 h; **b-1** 1 h; **c-1** 2.5 h; **d-1** 5.5 h. Consider HTMS adding moment as 0.

Effects of ammonia, water, and HTMS content on wettability and morphology of coatings

In our study, we found that the wetting properties and morphology of coatings changed with different concentration of ammonia, water, and HTMS. Considered study based on formulations of the modified silica sol shown in Tables 1 and 2.

Under the catalysis of ammonia (base), the Si–OR (R=CH_3 OR CH_2) was hydrolyzed and Si–OH was generated; then, the hydrolyzed siloxanes collided with each other and condensed into three-dimensional network and further reunited into particles via intermolecular force. As a result, gel or precipitate or

homogeneous modified silica sol could be formed due to different reaction conditions [37]. The hydrolysis rate increased as the catalyst concentration increased, and the resulting three-dimensional network got more highly cross-linked. Thus, polymers became denser and particles packed more tightly to form more hierarchical structure, which could be observed though SEM morphology of the coatings surfaces shown in Fig. 6a-1–4. Therefore, as ammonia content increased, water contact angle of the coatings increased obviously from 120° to 154° and water sliding angle decreased significantly from 90° to 5°

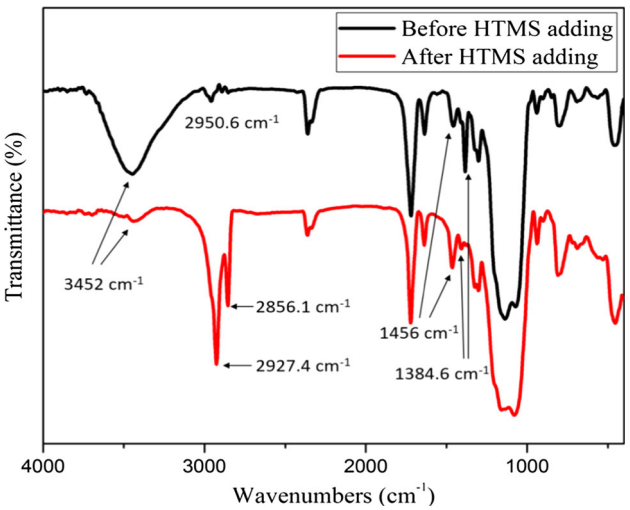

Figure 3 FTIR of coating surfaces before and after HTMS adding.

(Fig. 5a). Water drops could easily roll down from the surfaces. However, continuously increasing the concentration of ammonia resulted in severe agglomeration of the particles, which resulted in a light decrease in coating's water contact angle as well as increase in sliding angle. What is worse, the coating became brittle and cracks were obvious on the coating, which is shown in (Fig. 6a-4).

The change in water concentration had similar influences on wettability and morphology of coating surface. The water contact angle of coatings increased slightly from 146° to 158° as water concentration increased; meanwhile, the sliding angle decreased significantly from 90° to 1.8°, which is shown in Fig. 5b. Water concentration in this system was far more excessive than theoretical value though it was rather low (actual molar ratio of TEOS: MPS + HTMS: H_2O = 1: (0.76–1.42): (20.8–48.6), theoretical molar ratio of TEOS: MPS + HTMS: H_2O = 1: (0.76–1.42): (6.28–4.26), considered that siloxanes were totally hydrolyzed). Therefore, even the lowest water concentration could meet the need of hydrolysis. However, water concentration had a great influence on surfaces morphology shown in Fig. 6b-1–4. Dispersed rough particles with size of 3.12 ± 0.11 μm (measured by Image J, in Fig. 6b-1) could be observed at first. As shown in Fig. 6b-2–4, the particle size gradually decreased with the increase in water content, which was 0.34 ± 0.04 μm, 0.26 ± 0.02 μm, 0.19 ± 0.02 μm, respectively, furthermore, particles got closer and closer to form

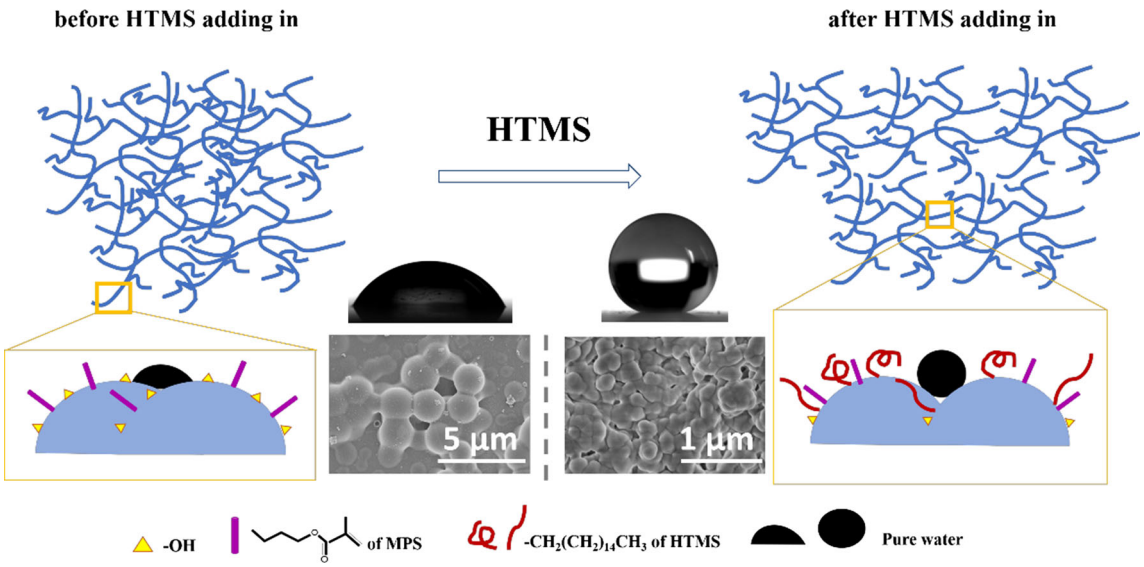

Figure 4 Schematic illustration of coating surfaces before and after HTMS adding.

Table 1 Formulation of different modified silica sol

Sample no.	TEOS/g	H_2O/g	EtOH/g	$NH_3{\cdot}H_2O$/ml	MPS/g	HTMS/g
1	1.663	5	45	1	1.167	0.909
2	1.663	5	45	1.5	1.167	0.909
3	1.663	5	45	2	1.167	0.909
4	1.663	5	45	2.5	1.167	0.909
5	1.663	5	45	3	1.167	0.909
6	1.663	5	45	2	1.167	0.4545
7	1.663	5	45	2	1.167	0.909
8	1.663	5	45	2	1.167	1.3635
9	1.663	5	45	2	1.167	1.818
10	1.663	5	45	2	1.167	2.2725
11	1.663	3	45	2	1.167	1.818
12	1.663	4	45	2	1.167	1.818
13	1.663	5	45	2	1.167	1.818
14	1.663	6	45	2	1.167	1.818
15	1.663	7	45	2	1.167	1.818

Table 2 Molar ratio of different modified silica sol[a]

Sample no.	TEOS/mol	H_2O/mol	$NH_3{\cdot}H_2O$/mol	MPS/mol	HTMS/mol
1	1	34.7	0.8	0.6	0.33
2	1	34.7	1.2	0.6	0.33
3	1	34.7	1.6	0.6	0.33
4	1	34.7	2	0.6	0.33
5	1	34.7	2.4	0.6	0.33
6	1	34.7	1.6	0.6	0.16
7	1	34.7	1.6	0.6	0.33
8	1	34.7	1.6	0.6	0.5
9	1	34.7	1.6	0.6	0.66
10	1	34.7	1.6	0.6	0.82
11	1	20.8	1.6	0.6	0.66
12	1	27.8	1.6	0.6	0.66
13	1	34.7	1.6	0.6	0.66
14	1	41.7	1.6	0.6	0.66
15	1	48.6	1.6	0.6	0.66

[a]Consider the molar mass of TEOS as 1 mol

hierarchical structure instead of loose spherical structure, which enabled the coatings to become more water repellent with higher water contact angle and lower sliding angle.

More importantly, the coatings surfaces' wettability and morphology were significantly affected by HTMS content. HTMS contains three hydrolysable methoxy groups and a long-chain alkane, which not only improved the roughness (shown in Fig. 5c) of the coating surface but provided hydrophobic group for the superhydrophobic coatings. With more HTMS addition, more –OH groups were grafted by long-chain alkane of HTMS and the hierarchical structure was constructed (Fig. 6c-1–4, Figure S1a–d); thus, the coating surfaces became more hydrophobic with the water contact angle increasing from 140° to 156.5° and the sliding angle decreasing from 55° to 5.1°, as shown in Fig. 5c. When the amount of HTMS was small, the morphology of corresponding coating was relatively flat (Fig. 6c-1, Figure S1a) with very small roughness of 43.8 nm, and the contact angle was low. With the increase in HTMS concentration, the hierarchical structure became obvious and kept similar morphology (Fig. 6c-2–3, Figure S1b–d) with a

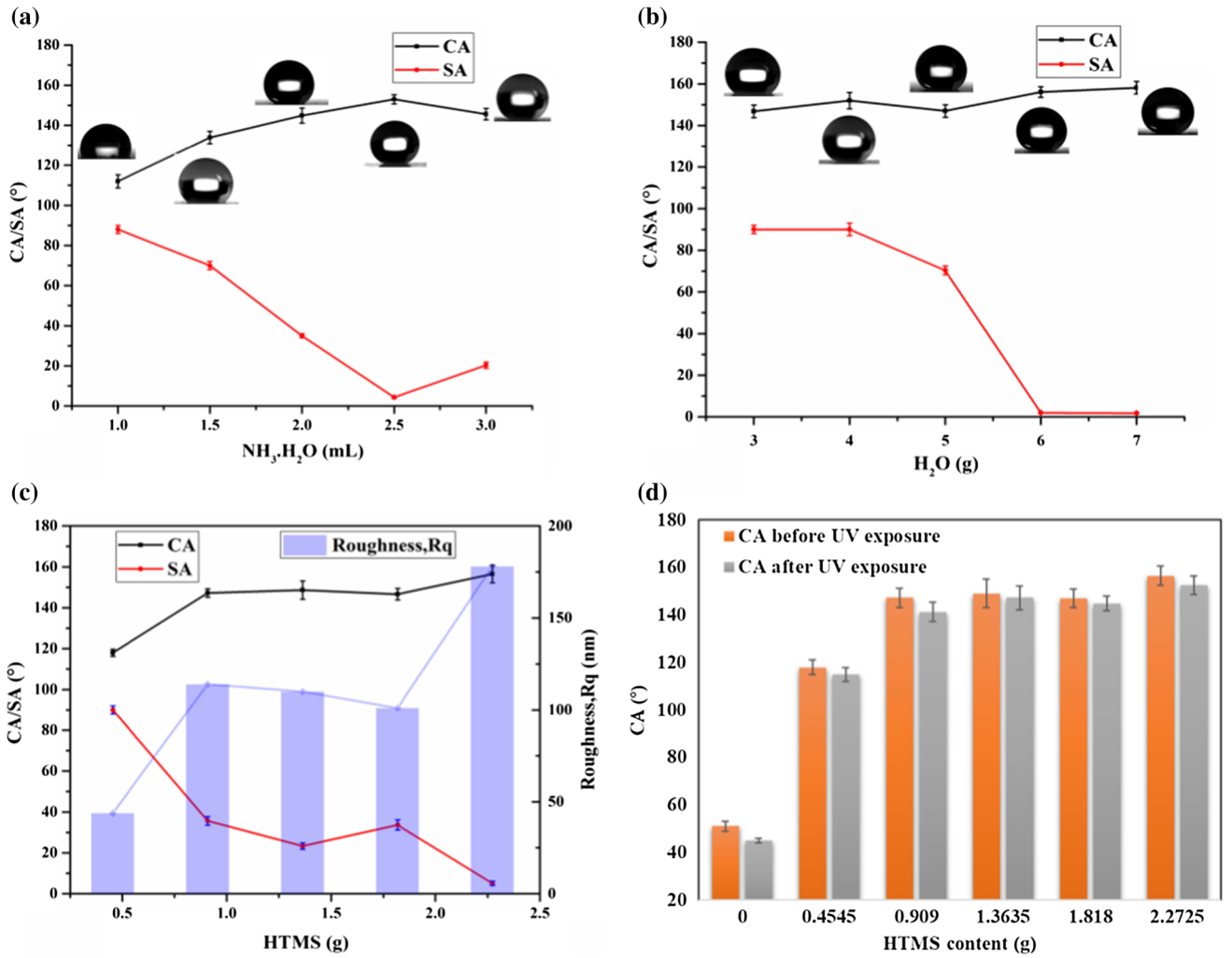

Figure 5 **a**–**c** Contact angle(CA)/sliding angle(SA) curve of different ammonia content, water content and HTMS content, respectively; **d** contact angle(CA)/sliding angle(CA) with different HTMS content before and after UV exposure.

roughness of about 110 nm (Fig. 5c). As the amount of HTMS further increasing, the roughness of the surface obviously increased to 178 nm and the great superhydrophobicity of coating was obtained. However, too more HTMS would lead to excessively packed particles as large scale of particles are shown in Fig. 6c-4, which directly led to crack of coatings. Besides, as more –OH replaced by long-chain alkane of HTMS, less –OH was left for bonding with substrates; thus, the formed coating's adhesion with substrate was rather weak.

In conclusion, to obtain a rather good superhydrophobic coating, the feed molar ratio could be TEOS/MPS/HTMS/H_2O/NH_3 = 1:0.6:0.66:41.7:0.6.

Effect of HTMS addition on durability of the coatings

To study the effect of HTMS addition on durability of the coatings, we employed UV exposure test and water impact test to evaluate physical resistance and acetic acid salt spray (AASS) test to evaluate coatings' chemical resistance.

For UV exposure test, standard ISO 4892-3:2016 (Plastics—Methods of exposure to laboratory light sources—Part 3: Fluorescent UV lamps) and a multifunctional device equipped with UV illumination, condensation and water jet system were adopted, which were used to evaluate humid environment including heat, light, rain, and dew. Samples with different HTMS content were tested. Exposure circle was set as follows: samples were first radiated under

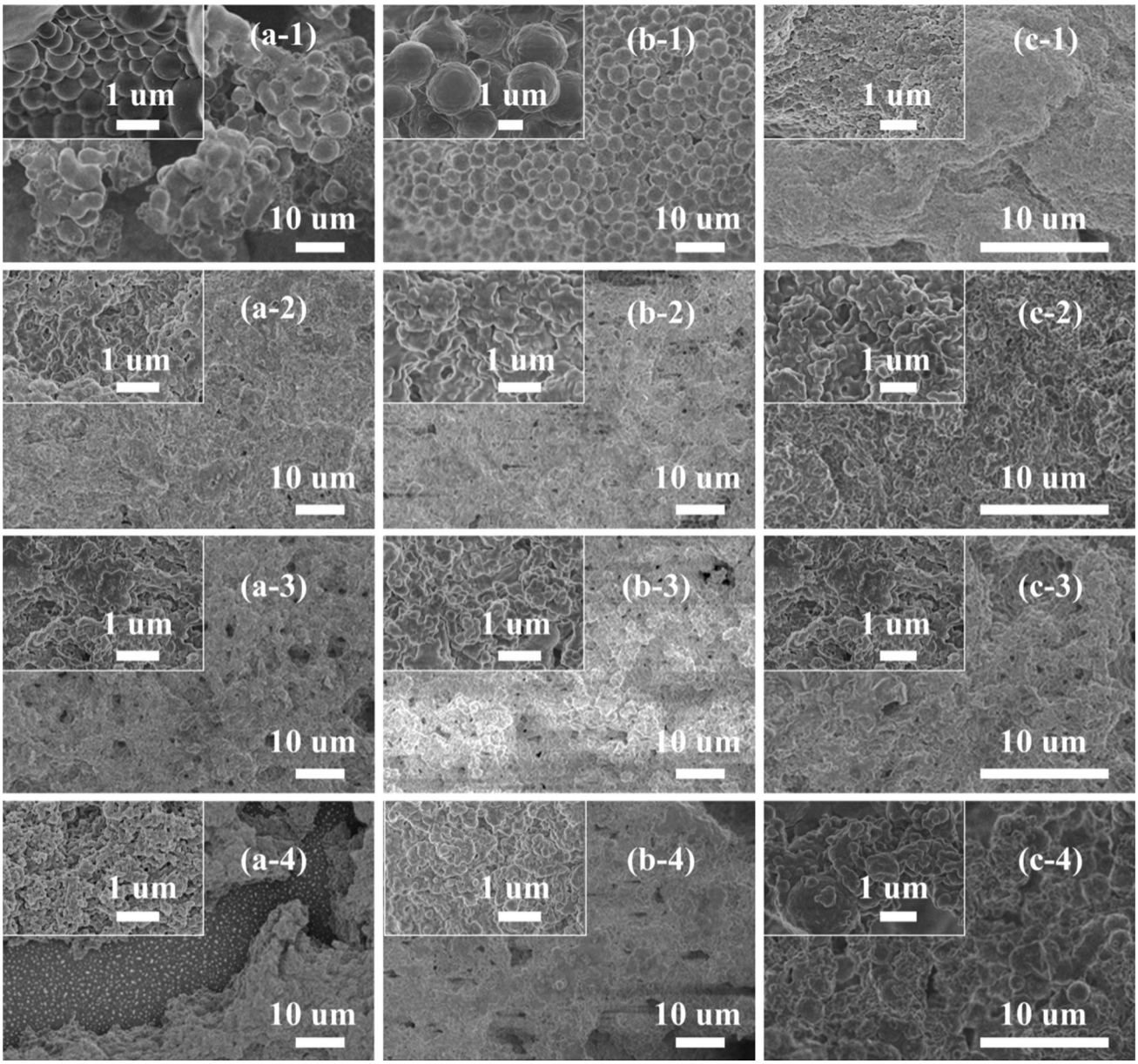

Figure 6 (**a-1**–**4**) Morphology via SEM of coatings with ammonia content (mass ratio) of 1.65, 3.24, 4.07, 4.78%, respectively; (**b-1**–**4**) morphology via SEM of coatings with water content (mass ratio) of 6.5, 8.0, 9.5, 11.0%, respectively; (**c-1**–**4**) morphology via SEM of coatings with HTMS content (mass ratio) of 0.7, 1.4, 2.1, 3.5%, respectively.

UVA-340 nm for 8 h at 50 °C and then were impacted by jet water under the same light at room temperature for another 0.25 h and then were heated at 50 °C without exposure for 3.75 h. The whole test lasted 10 circles. The contact angle of coatings before and after exposure (Fig. 5d) was measured. After UV exposure, the contact angles of coatings with different HTMS content all decreased slightly. However, these coatings still remained good hydrophobicity with CA > 135°. For coating without HTMS, the contact angle also decreased, but both were below 60° before and after UV exposure.

For water impact test, we employed a set of experimental device according to GB/T 10299-2011. The photograph of the device is shown in Figure S2. The sample was placed at a tilted angle of 45 °, and the sprayer was adjusted just above the coating. The water flow was stabilized at 100 L/h. Each coating sample was sprayed for continuous 5 h. After *t*, the coating was dried at 40 °C for 2 h; then, the contact

angle and the sliding angle of the coating were measured. For chemical resistance test, acetic acid salt spray (AASS) test (pH = 3) and base resistance test (pH = 14) were adopted. For acetic acid salt spray (AASS) test, ISO 9227:2017 (corrosion tests in artificial atmospheres—salt spray tests) was employed. Coatings were placed at a tilted angle of 60°, and acetic acid salt spray fell free onto the surface of the coatings for continuous 48 h. For base test, coatings were drawn in NaOH solution (pH = 14) for 5 h. The contact angle and sliding angle of the coating before and after test were measured. As shown in Fig. 7, even coatings suffered from water impact, acetic acid salt spray, and base for a long time, those with high content of HTMS still exhibit good superhydrophobicity, and the corresponding CA and SA changed slightly, indicating that HTMS could improve superhydrophobicity and the obtained coating might have a considerable durability when used in natural environment.

In order to further study the coating's abrasion resistance, a 1000-grit sandpaper was used. The sandpaper was placed on a horizontal tabletop, and the coating was brought into contact with the sandpaper. A 100-g weight was superimposed on the coating. The coating was pushed evenly in one direction for 50 cm and then was pushed in the vertical direction for another 50 cm. The total travel distance of the coating is 1 m. After abrasion, the water contact angle of the coating decreased to 130° (Fig. 8), which indicated that the coating's resistance to severe abrasion was not strong enough.

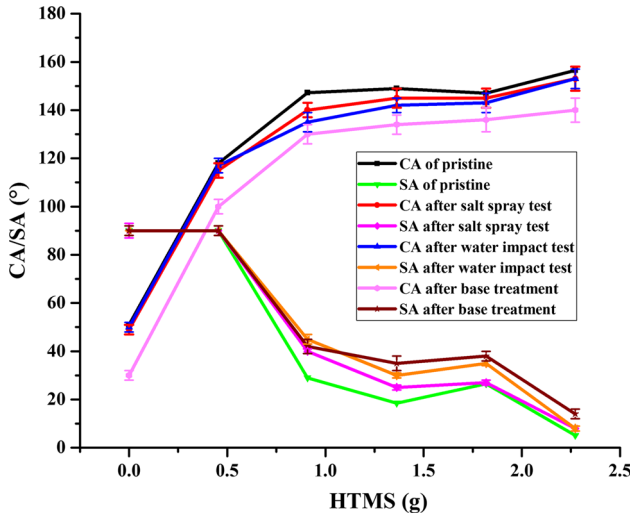

Figure 7 Contact angle (CA)/sliding angle (SA) before and after salt spray test/water impact test.

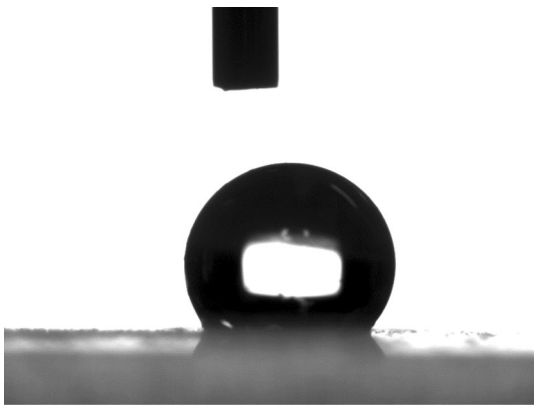

Figure 8 Contact angle (CA) after sandpaper abrasion for 1 m.

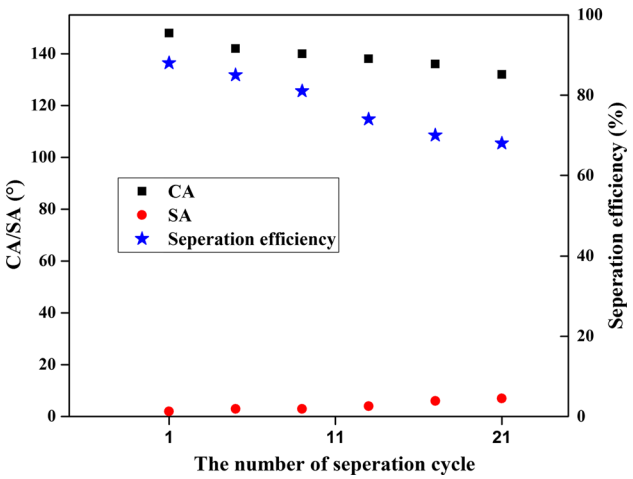

Figure 9 Contact angle/sliding angle/separation efficiency change with the number of separation cycle.

Table 3 Contact angle and sliding angle of coatings on different substrates

substrates	Contact angle/°	Sliding angle/°
Slides[a]	158	1.8
Tin foil paper	145	5
Tape (outer surface)	140	7
PET filter	149	2
Beaker (curved surface)[b]	–	1.6
Steel spoon (curved surface)[b]	–	1.7

[a]The best data of slides samples in this study; [b]the curved surfaces' contact angle is not important in this study, so we did not do the test

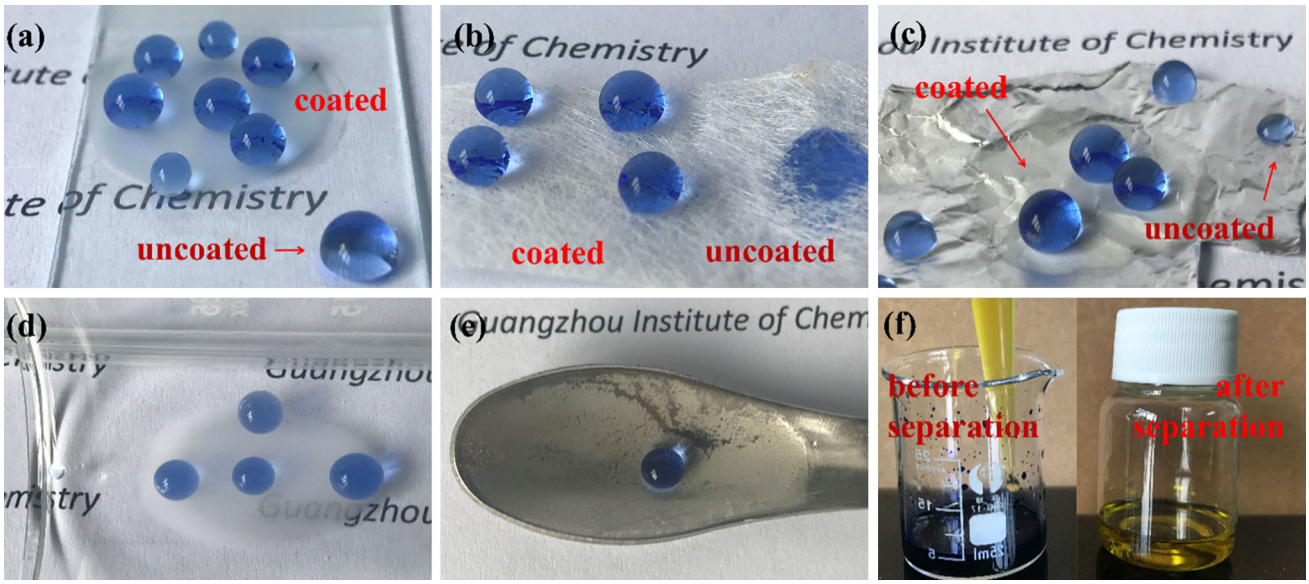

Figure 10 Digital images of pure water (stained with blue ink) on **a** slide; **b** PET filter; **c** tin foil paper; **d** beaker (inner surface); **e** steel spoon (inner surface); **f** before and after separation.

Wettability of coatings on other substrates

We also found that the modified silica sol could form superhydrophobic coatings on other substrates, and except for plain surfaces, superhydrophobicity worked well on curved surfaces, either. As shown in Fig. 9, superhydrophobicity worked well on both plain and curved surfaces with high contact angle and very low sliding angle, which is given in Table 3. (For corresponding videos, see supplementary 1–5.)

In addition, PET filter with superhydrophobic coating could be used to separate oil and water. In this study, we have tested its separation effect with olive oil and blue ink. The filter is put on a beaker mouth, 2.5 ml olive oil and 2.5 ml blue ink together are mixed and stirred for 30 s, and then the mixture is dripped onto the filter drop by drop. After 10 s, olive oil started to penetrate the filter and fell into the beaker. (For corresponding process, see supplementary 6.) The oil/water separation test was repeated for 21 times, and the contact angle, sliding angle, and separation efficiency were measured and calculated every four times. As shown in Fig. 9, after 21 cycles, the filter remained good hydrophobicity with CA of 132° and SA of 7°, and the separation efficiency decreased from 88 to 68%, indicating that the coated filter had a considerable recyclability. Appearances of olive oil before and after separation are shown in Fig. 10f.

Conclusions

In this work, a one-pot organic–inorganic hybrid modified silica sol and its coating with superhydrophobicity and chemical and UV resistance were successfully fabricated in a simple way. The modified silica sol could be self-leveling-coated or dip-coated on plain and curved surfaces of different substrates such as glass, metal, and polymer to form superhydrophobic coatings with a contact angle and a sliding angle of 158° and 1.8°, respectively. In addition, PET filter with this coating could be used to separate oil and water with a separation efficiency of 80%. The sol–gel process was studied. Under condition of low water content, the coatings' superhydrophobicity became better when the ammonia content, water content, and low-surface-energy material (HTMS) content were increased. However, too more ammonia or water or HTMS would sacrifice the coating's integrality and lead to the cracking of it.

Compliance with ethical standards

Conflicts of interest The authors declare that they have no conflict of interests.

Electronic supplementary material: The online version of this article (https://doi.org/10.1007/

s10853-018-2348-7) contains supplementary material, which is available to authorized users.

References

[1] Wang S, Jiang L (2007) Definition of superhydrophobic states. Adv Mater 19(21):3423–3424

[2] Marmur A (2004) The lotus effect: superhydrophobicity and metastability. Langmuir 20(9):3517–3519

[3] Wang Y, Xue J, Wang Q, Chen Q, Ding J (2013) Verification of icephobic/anti-icing properties of a superhydrophobic surface. ACS Appl Mater Interfaces 5(8):3370–3381

[4] Wang Z, Li Q, She Z, Chen F, Li L (2012) Low-cost and large-scale fabrication method for an environmentally-friendly superhydrophobic coating on magnesium alloy. J Mater Chem 22(9):4097–4105

[5] Xiu Y, Hess DW, Wong CP (2008) UV and thermally stable superhydrophobic coatings from sol–gel processing. J Colloid Interface Sci 326(2):465–470

[6] Tian Y, Guo K, Bian X, Sun J (2017) Durable and room-temperature curable superhydrophobic composite coating on nitrocellulose lacquer. Surf Coat Technol 325:444–450

[7] Ju J, Xiao K, Yao X, Bai H, Jiang L (2013) Bioinspired conical copper wire with gradient wettability for continuous and efficient fog collection. Adv Mater 25(41):5937–5942

[8] Zimmermann J, Reifler FA, Schrade U, Artus GRJ, Seeger S (2007) Long term environmental durability of a superhydrophobic silicone nanofilament coating. Colloids Surf A Physicochem Eng Asp 302(1–3):234–240

[9] Chen K, Zhou S, Yang S, Wu L (2015) Fabrication of all-water-based self-repairing superhydrophobic coatings based on UV-responsive microcapsules. Adv Funct Mater 25(7):1035–1041

[10] Zheng S, Li C, Fu Q et al (2016) Development of stable superhydrophobic coatings on aluminum surface for corrosion-resistant, self-cleaning, and anti-icing applications. Mater Des 93:261–270

[11] Su B, Tian Y, Jiang L (2016) Bioinspired interfaces with superwettability: from materials to chemistry. J Am Chem Soc 138(6):1727–1748

[12] Blossey R (2003) Self-cleaning surfaces—virtual realities. Nat Mater 2(5):301–306

[13] Feng X, Jiang L (2006) Design and creation of superwetting/antiwetting surfaces. Adv Mater 18(23):3063–3078

[14] Gao L, McCarthy TJ (2006) The "lotus effect" explained: two reasons why two length scales of topography are important. Langmuir 22(7):2966–2967

[15] Yan YY, Gao N, Barthlott W (2011) Mimicking natural superhydrophobic surfaces and grasping the wetting process: a review on recent progress in preparing superhydrophobic surfaces. Adv Colloid Interface Sci 169(2):80–105

[16] Deng X, Mammen L, Butt H-J, Vollmer D (2012) Candle soot as a template for a transparent robust superamphiphobic coating. Science 335(6064):67–70

[17] Zhang L, Wu J, Wang Y, Long Y, Zhao N, Xu J (2012) Combination of bioinspiration: a general route to superhydrophobic particles. J Am Chem Soc 134(24):9879–9881

[18] Du X, Liu X, Chen H, He J (2009) Facile fabrication of raspberry-like composite nanoparticles and their application as building blocks for constructing superhydrophilic coatings. J Phys Chem C 113(21):9063–9070

[19] Cortese B, D'Amone S, Manca M, Viola I, Cingolani R, Gigli G (2008) Superhydrophobicity due to the hierarchical scale roughness of PDMS surfaces. Langmuir 24(6):2712–2718

[20] Lv T, Cheng Z, Zhang E, Kang H, Liu Y, Jiang L (2016) Self-restoration of superhydrophobicity on shape memory polymer arrays with both crushed microstructure and damaged surface chemistry. Small 13(4):1503402

[21] Li F, Du M, Zheng Q (2016) Dopamine/silica nanoparticle assembled, microscale porous structure for versatile superamphiphobic coating. ACS Nano 10(2):2910–2921

[22] Koch K, Bhushan B, Jung YC, Barthlott W (2009) Fabrication of artificial Lotus leaves and significance of hierarchical structure for superhydrophobicity and low adhesion. Soft Matter 5(7):1386–1393

[23] Ma M, Mao Y, Gupta M, Gleason KK, Rutledge GC (2005) Superhydrophobic fabrics produced by electrospinning and chemical vapor deposition. Macromolecules 38(23):9742–9748

[24] Lu X, Wang C, Wei Y (2009) One-dimensional composite nanomaterials: synthesis by electrospinning and their applications. Small 5(21):2349–2370

[25] Wu L, Li L, Li B, Zhang J, Wang A (2015) Magnetic, durable, and superhydrophobic polyurethane@Fe3O4@SiO2@fluoropolymer sponges for selective oil absorption and oil/water separation. ACS Appl Mater Interfaces 7(8):4936–4946

[26] Pereira C, Alves C, Monteiro A et al (2011) Designing novel hybrid materials by one-pot co-condensation: from hydrophobic mesoporous silica nanoparticles to superamphiphobic cotton textiles. ACS Appl Mater Interfaces 3(7):2289–2299

[27] Li F, Du M, Zheng Z, Song Y, Zheng Q (2015) A facile, multifunctional, transparent, and superhydrophobic coating based on a nanoscale porous structure spontaneously assembled from branched silica nanoparticles. Adv Mater Interfaces 2(13):1500201

[28] Zhu T, Cai C, Guo J, Wang R, Zhao N, Xu J (2017) Ultra water repellent polypropylene surfaces with tunable water adhesion. ACS Appl Mater Interfaces 9(11):10224–10232

[29] Xie Q, Xu J, Feng L et al (2004) Facile creation of a super-amphiphobic coating surface with bionic microstructure. Adv Mater 16(4):302–305

[30] Osborne JH (2001) Observations on chromate conversion coatings from a sol–gel perspective. Prog Org Coat 41(4):280–286

[31] Poovarodom S, Hosseinpour D, Berg JC (2008) Effect of particle aggregation on the mechanical properties of a reinforced organic–inorganic hybrid sol–gel composite. Ind Eng Chem Res 47(8):2623–2629

[32] Simpson JT, Hunter SR, Aytug T (2015) Superhydrophobic materials and coatings: a review. Rep Prog Phys 78(8):086501

[33] Bayer I (2017) On the durability and wear resistance of transparent superhydrophobic coatings. Coatings 7(12):12

[34] Stöber W, Fink A, Bohn E (1968) Controlled growth of monodisperse silica spheres in the micron size range. J Colloid Interface Sci 26(1):62–69

[35] Diré S, Babonneau F, Sanchez C, Livage J (1992) Sol–gel synthesis of siloxane oxide hybrid coatings $[Si(CH_3)_2$-O·MOX–M=Si, Ti, Zr, Al] with luminescent properties. J Mater Chem 2(2):239–244

[36] Crivello JV, Mao Z (1997) Synthesis of novel multifunctional siloxane oligomers using sol–gel techniques and their photoinitiated cationic polymerization. Chem Mater 9(7):1554–1561

[37] Buckley AM, Greenblatt M (1994) The sol–gel preparation of silica gels. J Chem Edu 71(7):599–602